

## Kinetics of $\text{Fe}_2\text{O}_3$ -Al reaction prior to mechanochemical synthesis of $\text{Fe}_3\text{Al-Al}_2\text{O}_3$ nanocomposite powder using thermal analysis

M. Khodaei

Faculty of Materials Science and Engineering, K.N. Toosi University of Technology, Tehran, Iran

Received: 2019-05-07

Accepted: 2019-05-22

Published: 2019-06-20

### ABSTRACT

The effect of ball milling on kinetics of the thermite reaction of  $3\text{Fe}_2\text{O}_3 + 8\text{Al}$  powder mixture to synthesize  $\text{Fe}_3\text{Al-Al}_2\text{O}_3$  nanocomposite was investigated using differential thermal analysis. A model-free method was applied to the non-isothermal differential calorimetry (DSC) data to evaluate the reaction kinetics according to the Starink method. The activation energy of the thermite reaction in the  $\text{Fe}_2\text{O}_3$ -Al system in ball milled  $3\text{Fe}_2\text{O}_3 + 8\text{Al}$  powder mixture was determined to be 97 kJ/mole, which is smaller than that for non-milled powder mixture indicating the change of reaction mechanisms. The change in the reaction mechanism could be resulted from the formation of short-circuit diffusion paths occurring in the precursors during milling. The change in the reaction mechanism of such nanostructured  $3\text{Fe}_2\text{O}_3 + 8\text{Al}$  powder mixture could be reason of the formation of desired phases ( $\text{Fe}_3\text{Al}$  and  $\text{Al}_2\text{O}_3$ ), which such stoichiometric phases cannot be achieved by conventional molten state thermite reaction.

**Keywords:** Differential Scanning Calorimetry (DSC);  $\text{Fe}_3\text{Al-Al}_2\text{O}_3$ ; Kinetics; Mechanochemical; Nanocomposite  
© 2019 Published by Journal of Nanoanalysis.

### How to cite this article

Khodaei M. Kinetics of  $\text{Fe}_2\text{O}_3$ -Al reaction prior to mechanochemical synthesis of  $\text{Fe}_3\text{Al-Al}_2\text{O}_3$  nanocomposite powder using thermal analysis. J. Nanoanalysis., 2019; 6(3): 199-204. DOI: 10.22034/jna.\*\*\*

## INTRODUCTION

Various techniques have been introduced for fabrication of metal/ceramic composites, which are based on ex-situ processes (addition of reinforcement to the matrix) such as convectional powder metallurgy and casting techniques or in-situ processes (direct fabrication of reinforcement in the matrix) such as direct metal oxidation, reactive melt penetration, reactive sintering, and self-propagating high-temperature synthesis (SHS) [1, 2].

The in-situ processes can economically fabricate a significantly wider range of interpenetrating phase composites. In order to synthesis the metal(intermetallic)/alumina composite, the in-situ reaction between metal oxide and elemental aluminum could be utilized using various methods such as aluminothermic reaction [3] and mechanochemical reaction [4]. Synthesis of  $\text{Fe}(\text{Al})/$

$\text{Al}_2\text{O}_3$  composite by aluminothermic reaction [5] and mechanochemical reaction [6,7] has been investigated. The kinetics of thermite reaction of  $3\text{Fe}_2\text{O}_3 + 8\text{Al}$  powder mixture in molten state to synthesize  $\text{Fe}_3\text{Al}/\text{Al}_2\text{O}_3$  composite was investigated by Fan et al. [5]. The theoretical as well as experimental investigations revealed that  $\text{FeAl}_2\text{O}_4$  phase was obtained instead of thermodynamically predicted  $\text{Fe}_3\text{Al}$  phase during the reaction of molten Al with  $\text{Fe}_2\text{O}_3$  [5].

In our previous works [7, 8],  $\text{Fe}_3\text{Al}/\text{Al}_2\text{O}_3$  nanocomposite was successfully synthesized by mechanochemical reaction of  $3\text{Fe}_2\text{O}_3 + 8\text{Al}$  powder mixture. In this paper, the kinetics aspect of mechanically activated  $3\text{Fe}_2\text{O}_3 + 8\text{Al}$  powder mixture was investigated by differential scanning calorimetry (DSC) in order to reveal the capability of mechanochemical process rather than thermite reaction to synthesize  $\text{Fe}_3\text{Al}/\text{Al}_2\text{O}_3$  composite.

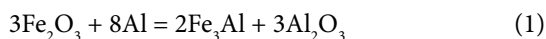
\* Corresponding Author Email: [khodaei@kntu.ac.ir](mailto:khodaei@kntu.ac.ir)



## EXPERIMENTAL

### Experimental methods

Fe<sub>2</sub>O<sub>3</sub> (99.9% purity) and Al (99.5% purity) were mixed according to the following reaction.



Ball milling of powder mixture was carried out in a Spex8000 type ball mill. The vial rotation speed and its vibration frequency were 700 rpm and 11.7 Hz, respectively. The milling media were hardened chromium steel consisted of five 12 mm diameter balls, confined in a 75 ml volume vial. A total powder of 7 g without any process control agent was milled under argon atmosphere. The ball-to-powder weight ratio was 5:1. The phase composition of samples was investigated by X-ray diffractometry (XRD) using a Philips X'PERT MPD diffractometer with Cu K<sub>α</sub> radiation (λ=0.15418 nm). Differential scanning calorimetry (DSC) was carried out in a Q100 V9/4 Build 287 thermal analyzer under flowing argon atmosphere in alumina crucibles within a temperature range of 30-1200 °C, applying different heating rate from 5 to 20 °C/min.

### Theoretical methods

Kinetics of thermally activated solid state reaction has been widely investigated by following a formula:

$$d\alpha/dt = k(T) \cdot f(\alpha) = A \exp(-E_a/RT) \cdot f(\alpha) \quad (2)$$

Where  $\alpha$  is the extent of reaction (conversion degree);  $t$ , the time;  $R$ , universal gas constant;  $T$ , temperature;  $f(\alpha)$ , kinetic model function;  $A$  and  $E_a$  are Arrhenius parameters, apparent pre-exponential factor and apparent activation energy, respectively.

Two approaches that used in kinetic evolutions are model-fitting and model-free methods. In model-fitting methods, a kinetic model can be assumed to describe the reaction behavior for both isothermal and non-isothermal kinetic evolutions. By fitting the experimental data to different assumed model function  $f(\alpha)$ , the overall reaction is described by the combination of formal reaction steps with constant Arrhenius parameters, which are determined by choosing the form of  $f(\alpha)$ . However, in a non-isothermal experiments both  $T$  and  $\alpha$  vary simultaneously, the model-fitting methods generally fail to achieve accurate

separation between  $k(T)$  and  $f(\alpha)$  functions. As a result, any  $f(\alpha)$  can satisfactorily fit data at a cost of drastic variations in Arrhenius parameters, which compensate for the difference between the assumed form of  $f(\alpha)$  and the true but unknown reaction model. Consequently, the model-fitting method leads to achieving the uncertain values of Arrhenius parameters [9].

In model-free method, the Arrhenius parameters could be determined without choosing the reaction model. The well known approaches, if several measurements with different heating rates and/or with different temperatures are performed, are the isoconversional method according to the Friedman and the integral isoconversional method according to the Kissinger and Ozawa [9]. For non-isothermal analysis at constant heating rate, mean activation energy can be derived using Kissinger-type isoconversional methods. However, these methods are subject to approximations which can introduce inaccuracies in the determination of  $E_a$ . A new method for the derivation of activation energy is proposed by Starink [10]. It is shown that this method is more accurate than the Kissinger and Ozawa methods.

A comparison of the Kissinger-type methods shows that they all comply with the following equation:

$$\ln(T_p^s / \varphi) = A(E_a / RT_p) + \text{constant} \quad (3)$$

Where  $T_p$  is the peak temperature of DSC curve;  $\varphi$ , is the heating rate;  $s$ , is a constant, and  $A$  is a constant which depends on a choice of  $s$ . In the case of Kissinger method,  $s = 2$  and  $A = 1$ , and for Ozawa method  $s = 0$  and  $A = 1.0518$ , while for the Starink method  $s = 1.8$  and  $A = 1.007-1.2 \times 10^{-5} E_a$  ( $E_a$  in kJ/mol). The activation energy,  $E_a$ , can be determined from a plot of  $\ln(T_p^s / \varphi)$  versus of  $1/T_p$ .

## RESULTS AND DISCUSSION

The 3Fe<sub>2</sub>O<sub>3</sub> + 8Al reaction is thermodynamically favorable giving Fe<sub>3</sub>Al and Al<sub>2</sub>O<sub>3</sub> phases. Fan and al. [5] reported that during reaction of Fe<sub>2</sub>O<sub>3</sub> and molten aluminum, instead of thermodynamically predicted Fe<sub>3</sub>Al intermetallic compound, FeAl<sub>2</sub>O<sub>4</sub> is predominately formed and thermite reaction in 3Fe<sub>2</sub>O<sub>3</sub> + 8Al powder mixture resulted in the formation of Al<sub>2</sub>O<sub>3</sub> and FeAl<sub>2</sub>O<sub>4</sub>. It has been revealed [5] that the activation energy for the thermite reaction in 3Fe<sub>2</sub>O<sub>3</sub> + 8Al powder mixture is near to that for the diffusion of Al into FeAl<sub>2</sub>O<sub>4</sub>

phase. Hence, the formation of  $\text{FeAl}_2\text{O}_4$  phase at  $\text{Fe}_2\text{O}_3/\text{Al}$  interfaces, controls the rate of reaction. Khodaei and et al [7, 8] reported that the  $\text{Fe}_3\text{Al}$  and  $\text{Al}_2\text{O}_3$  phases were successfully synthesized by mechanochemical reaction of  $3\text{Fe}_2\text{O}_3 + 8\text{Al}$  powder mixture. The calculated adiabatic temperature ( $T_{ad}$ ) [7] as well as experimental observations [8] revealed that the mechanochemical reaction of  $3\text{Fe}_2\text{O}_3 + 8\text{Al}$  powder mixture occurs with a combustion mode in which all expected phase,  $\text{Fe}_3\text{Al}$  and  $\text{Al}_2\text{O}_3$ , are achieved.

The XRD patterns of  $3\text{Fe}_2\text{O}_3 + 8\text{Al}$  powder mixture as-received and after different ball milling times are shown in Fig. 1. XRD pattern of powder mixture after 2 h of milling time (prior to combustion reaction, Fig. 1(b)) was identified as a mixture of  $\text{Fe}_2\text{O}_3$  and Al indicated that ball milling up to 2 h had no effect on as-received powder mixture except broadening of Bragg peaks resulting from nanocrystallization as well as the enhancement of lattice strain. XRD pattern taken immediately after combustion (by recording the vial temperature during ball milling [8]), Fig. 1(c), showed no  $\text{Fe}_2\text{O}_3$  and Al peaks. The diffraction peaks of reaction products were identified as  $\alpha\text{-Al}_2\text{O}_3$  and disordered  $\text{Fe}_3\text{Al}$  intermetallic compound. Although, the trace of Fe peak can be observed in XRD pattern, the peaks related to the  $\text{FeAl}_2\text{O}_4$  phase were not detected. These results are in contrast with the results of the thermite reaction of  $3\text{Fe}_2\text{O}_3 + 8\text{Al}$  [5] where the molten Al reacts with  $\text{Fe}_2\text{O}_3$  and the undesired  $\text{FeAl}_2\text{O}_4\text{-Al}_2\text{O}_3$  phases were obtained.

In order to evaluate the effect of mechanical activation on kinetics of  $\text{Fe}_2\text{O}_3\text{-Al}$  reaction, the

$3\text{Fe}_2\text{O}_3 + 8\text{Al}$  powder mixture after 2 h of ball milling (before starting the combustion reaction during milling) was heated in DSC. The activation energy of the reaction was obtained according to the Starink method [10].

Fig. 2 shows the DSC curves of 2 h ball milled  $3\text{Fe}_2\text{O}_3 + 8\text{Al}$  powder mixture at different heating rates. As can be seen, all curves have similar peaks including two exothermic peaks and one endothermic peak. The endothermic peak at about  $660^\circ\text{C}$  is related to the melting of Al. In order to determine the first exothermic peak, the 2 h ball milled  $3\text{Fe}_2\text{O}_3 + 8\text{Al}$  powder mixture was heated up to  $600^\circ\text{C}$  with a heating rate of  $10^\circ\text{C}/\text{min}$ . The XRD pattern of the 2 h ball milled  $3\text{Fe}_2\text{O}_3 + 8\text{Al}$  powder mixture before and after heating up to  $600^\circ\text{C}$  are shown in Fig. 3. Fig. 3(b) consisted of the  $\text{Al}_2\text{O}_3$ ,  $\text{Fe}_3\text{Al}$ ,  $\text{Fe}_2\text{O}_3$ , and Al peaks. The first exothermic peak is therefore related to the solid state reaction of  $\text{Fe}_2\text{O}_3$  and Al at about  $600^\circ\text{C}$ . On DSC curve of  $3\text{Fe}_2\text{O}_3 + 8\text{Al}$  powder mixture without ball milling, this exothermic peak occurred after melting of Al at about  $900^\circ\text{C}$  [5]. The second exothermic peaks at around  $800^\circ\text{C}$  on DSC curves may be due to the reaction of remaining Al and  $\text{Fe}_2\text{O}_3$ .

As mentioned in section 2-2, the activation energy ( $E_a$ ) could be determined from the slope of the Starink plot. Fig. 4 shows the Starink plot of  $\ln(T_p^{1.8}/\phi)$  versus  $1/T_p$  for the first exothermic peak. The activation energy of 2 h ball milled  $3\text{Fe}_2\text{O}_3 + 8\text{Al}$  powder mixture was measured to be about  $97\text{ kJ}/\text{mole}$ .

The first exothermic peak on DSC curves of  $3\text{Fe}_2\text{O}_3 + 8\text{Al}$  powder mixture decreased from

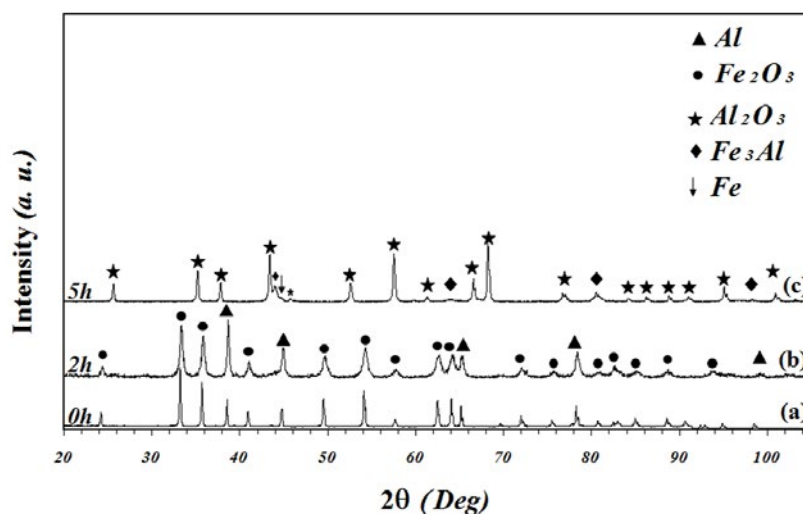


Fig. 1. XRD patterns of  $3\text{Fe}_2\text{O}_3 + 8\text{Al}$  powder mixture as-received and after different milling time.

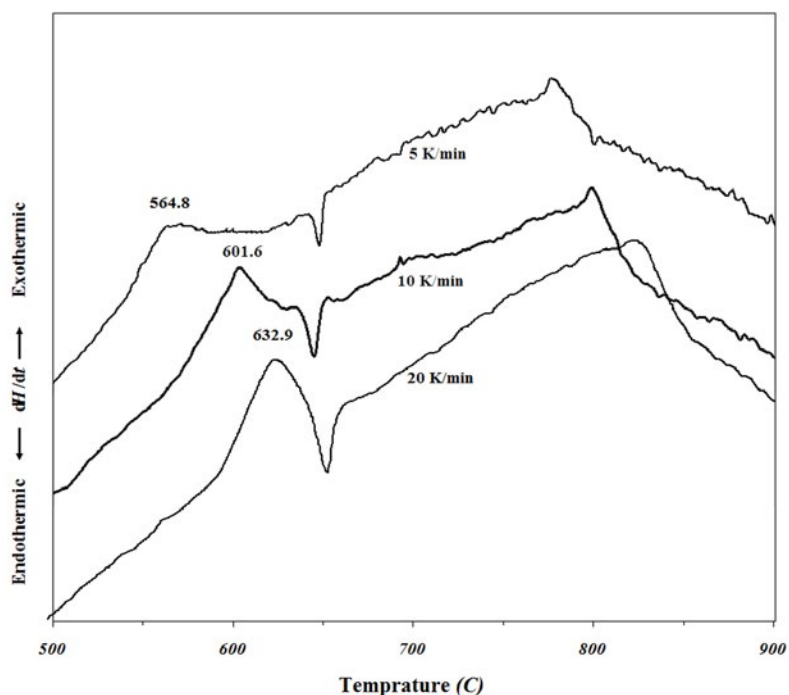


Fig. 2. DSC curves of 2 h ball milled  $3\text{Fe}_2\text{O}_3 + 8\text{Al}$  powder mixture at different heating rates.

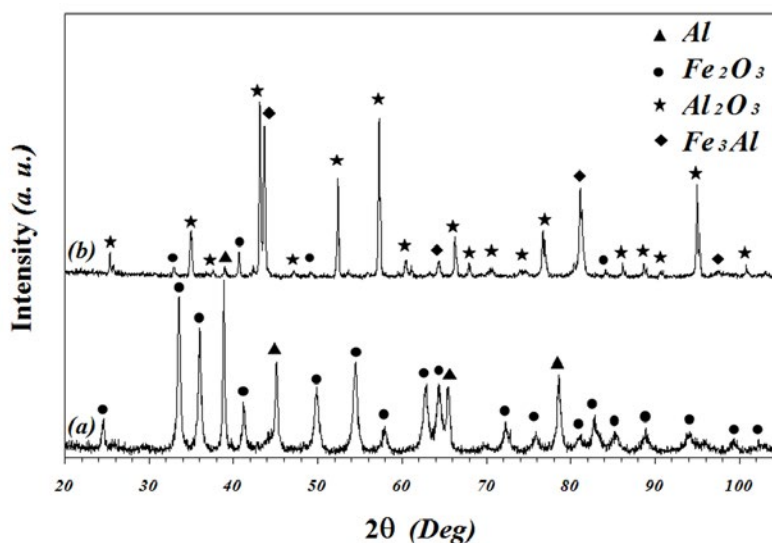


Fig. 3. XRD pattern of 2 h ball milled  $3\text{Fe}_2\text{O}_3 + 8\text{Al}$  powder mixture (a) as-milled, and (b) after subsequent heating up to  $600\text{ }^\circ\text{C}$ .

about  $900\text{ }^\circ\text{C}$  for unmilled powder [5] to about  $600\text{ }^\circ\text{C}$  for ball milled powder mixture. Also  $E_a$  of unmilled  $3\text{Fe}_2\text{O}_3 + 8\text{Al}$  powder mixture, calculated by Starink method, was reported to be about  $145\text{ kJ/mole}$  [5], whereas in ball milled powder mixture, the  $E_a$  reduced to the  $97\text{ kJ/mole}$ . These results indicate that the reaction mechanism of  $3\text{Fe}_2\text{O}_3 + 8\text{Al}$  powder mixture is changed as a result of ball

milling. Similar results are found in case of  $\text{CuO-Fe}$  reaction, which has been reported [11] that  $E_a$  of unmilled  $5\text{CuO} + 4\text{Fe}$  powder mixture was about  $575\text{ kJ/mole}$  which reduced gradually during ball milling to about  $200\text{ kJ/mole}$  prior to combustion. Investigation of microstructural changes during ball milling of  $3\text{Fe}_2\text{O}_3 + 8\text{Al}$  powder mixture revealed [8] that the crystallite size and mean lattice strain

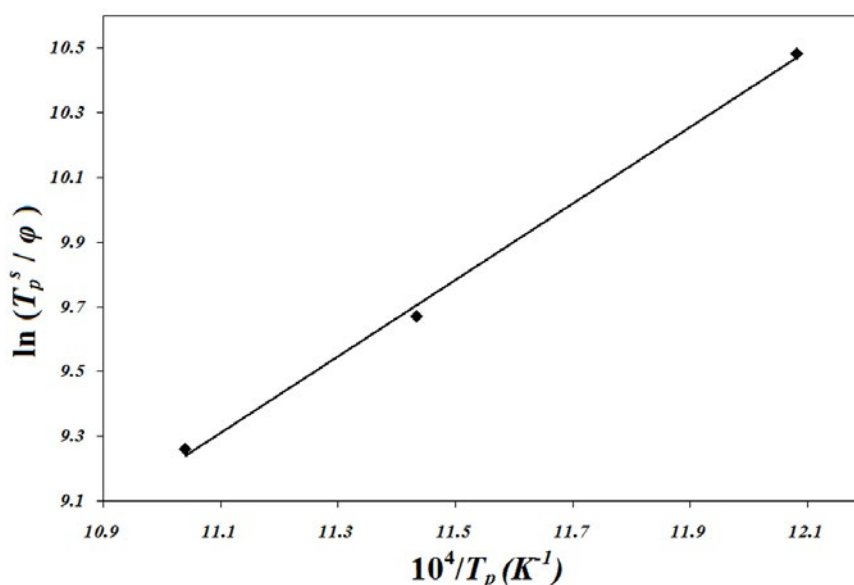


Fig. 4. Starink plot for the first exothermic peak of DSC curves

of  $\text{Fe}_2\text{O}_3$  and Al after 2 h of milling time became to 77nm, 0.8% and 81nm, 0.41%, respectively. Reducing the crystallite size to nanometer range and increasing the defect densities increase the reaction rate by providing short-circuit diffusion paths [12]. This nanostructured composite of  $\text{Fe}_2\text{O}_3$  and Al layer before ignition may be caused by the formation of predicted  $\text{Fe}_3\text{Al}$  phase. The results of molecular dynamics (MD) simulations of the planar interfacial contact of Al/ $\text{Fe}_2\text{O}_3$  nanolaminate thermite systems reported by Lin et. al. [13] revealed this hypothesis. They defined that the reaction will start when the initial distance among reactants is shorter than a certain distance after passing through the ignition delay. Moreover, Sui et. al. [14] revealed experimentally that the ignition of Al and  $\text{Fe}_2\text{O}_3$  layers is closely associated with oxygen which is produced from thermal decomposition of  $\text{Fe}_2\text{O}_3$  and the thickness of the reaction zone is restricted by the diffusion length of oxygen across the layer-to-layer interface of Al and  $\text{Fe}_2\text{O}_3$ , suggesting the benefit of nano-scale structure in such combustion system.

It was proposed by Forrester and Schaffer [11] that in unmilled powder mixture, the bulk ionic diffusion in oxide phase is rate-controlling of the reaction, subsequently, diffusion along grain boundaries and ionic short-circuit diffusion paths control the reaction in ball milled powder mixture, which is supported by dynamic molecular simulation [13] and experimental analysis [14].

It seems that the introducing the short-circuit diffusion paths by increasing the structural defect densities plays an important role in changing the reaction mechanism. In nanostructured powder mixture in which reactants are uniformly mixed at atomic scale, the diffusion mode has been changed. For ball milled powder mixture, the  $\text{Fe}_2\text{O}_3$ -Al reaction takes place before melting of Al in the solid state, whereas, for unmilled  $3\text{Fe}_2\text{O}_3 + 8\text{Al}$  powder mixture this reaction occurs after melting of Al [5]. These observations along with suddenly combustional synthesis of  $\text{Fe}_3\text{Al}/\text{Al}_2\text{O}_3$  nanocomposite during mechanochemical reaction of  $3\text{Fe}_2\text{O}_3 + 8\text{Al}$  powder mixture [7, 8] suggest that during ball milling process, the attainment of the critical combustion condition depends on the developments of an excess short-circuit diffusion paths and reducing the activation energy to occurring the sudden reaction. Hence, for ball milled  $3\text{Fe}_2\text{O}_3 + 8\text{Al}$  powder mixture the metal ionic diffusion (diffusion of Al in  $\text{FeAl}_2\text{O}_4$ ) that proposed by Fan and et al. [5] does not occur and the changing of ionic diffusion mode result in formation of desired phases.

## CONCLUSION

The effect of ball milling on kinetics of  $\text{Fe}_2\text{O}_3$ -Al reaction for mechanically activated  $3\text{Fe}_2\text{O}_3 + 8\text{Al}$  powder mixture was investigated in order to reveal the influence of mechanical activation on reaction mechanism. The activation energy

of 2 h ball milled  $3\text{Fe}_2\text{O}_3 + 8\text{Al}$  powder mixture (prior to combustion during mechanochemical synthesizing the  $\text{Fe}_3\text{Al}/\text{Al}_2\text{O}_3$  nanocomposite) was determined by non-isothermal differential scanning calorimetry performed at different heating rate using Starink method. The activation energy of  $\text{Fe}_2\text{O}_3$ -Al reaction for ball milled  $3\text{Fe}_2\text{O}_3 + 8\text{Al}$  powder mixture is measured to be 97 kJ/mole, which is smaller than that for unmilled powder mixture reported elsewhere, indicating the change in reaction mechanism. It seems that ball milling cause to nanocrystallization of precursor powders providing the short-circuit diffusion paths to enhance their reaction ability resulted in formation of desired phases,  $\text{Fe}_3\text{Al}$  and  $\text{Al}_2\text{O}_3$ . Such desired and stoichiometric products could be resulted from the nanostructured  $3\text{Fe}_2\text{O}_3 + 8\text{Al}$  powder mixture, whereas the conventional molten state thermite reaction has not such capability.

#### CONFLICT OF INTEREST

The authors declare that there is no conflict of interests regarding the publication of this manuscript.

#### REFERENCES

- [1] C. Suryanarayana, Mechanical alloying and milling, *Prog. Mater. Sci.* 46 (2001) 1–184.
- [2] R. Casati, M. Vedani, Metal Matrix Composites Reinforced by Nano-Particles—A Review, *Metals*, 4 (2014) 65-83.
- [3] H.X. Zhu, R. Abbaschian, In-situ processing of NiAl–alumina composites by thermite reaction *Mater. Sci. & Eng. A* 282 (2000) 1-7.
- [4] B.S.B. Reddy, K. Rajasekhar, M. Venu, J.J.S. Dilip, S. Das, K. Das, Mechanical activation-assisted solid-state combustion synthesis of in situ aluminum matrix hybrid ( $\text{Al}_3\text{Ni}/\text{Al}_2\text{O}_3$ ) nanocomposites, *J. Alloys & Comp.* 465 (2008) 97-105.
- [5] R.H. Fan, H.L. Lu, K.N. Sun, W.X. Wang, X.B. Yi, Kinetics of Thermite Reaction in Fe- $\text{Al}_2\text{O}_3$  System, *Thermochim. Acta* 440 (2006) 129-131.
- [6] D. Oleszak, M. Krasnowski, Mechanically alloyed nanocrystalline intermetallic matrix composite reinforced with alumina, *Mater. Sci. Forum* 360-362 (2001) 235-240.
- [7] M. Khodaei, M.H. Enayti, F. Karimzadeh, Mechanochemical behavior of  $\text{Fe}_2\text{O}_3$ -Al-Fe powder mixtures to produce  $\text{Fe}_3\text{Al}-\text{Al}_2\text{O}_3$  nanocomposite powder, *J Mater. Sci.* 43 (2008) 132-138.
- [8] M. Khodaei, M.H. Enayti, F. Karimzadeh, Mechanochemically synthesized  $\text{Fe}_3\text{Al}-\text{Al}_2\text{O}_3$  nanocomposite, *J. Alloys & Comp.* 467 (2009) 159-162.
- [9] S. Vyazovkin, C.A. Wight, Model-free and model-fitting approaches to kinetic analysis of isothermal and nonisothermal data, *Thermochim. Acta* 340–341 (1999) 53-68.
- [10] M.J. Starink, A new method for the derivation of activation energies from experiments performed at constant heating rate, *Thermochim. Acta* 288 (1996) 97-104.
- [11] J.S. Forrester, G.B. Schaffer, The chemical kinetics of mechanical alloying, *Metall. Trans. A* 26 (1995) 725-730.
- [12] G.B. Schaffer, P.G. McCormick, Displacement Reactions during Mechanical Alloying, *Metall. Trans. A* 21 (1990) 2789-2794.
- [13] L.Z. Lin, X.L. Cheng, B. Ma, Reaction characteristics and iron aluminides products analysis of planar interfacial Al/ $\alpha$ - $\text{Fe}_2\text{O}_3$  nanolaminate, *Computational Materials Science* 127 (2017) 29-41.
- [14] H. Sui, S. Atashin, J.Z. Wen, Thermo-chemical and energetic properties of layered nano-thermite composites, *Thermochimica Acta* 642 (2016) 17-24.